PICTORIAL ESSAY

Gastrointestinal stromal tumors (GISTs): an imaging perspective

Shahina Bano · Sunil Kumar Puri ·
Lalendra Upreti · Vikas Chaudhary ·
Hridesh Kumar Sant · Ranjana Gondal

Abstract Gastrointestinal stromal tumors (GISTs) are the most common mesenchymal tumors of the gastrointestinal tract. Computed tomography is the imaging modality of choice for diagnosing GIST. The aim of this retrospective study was to review the imaging features of 22 GIST cases. We also describe the clinical and pathological findings of this well-recognized entity.

Keywords Gastrointestinal stromal tumor (GIST) · Computed tomography (CT) · Magnetic resonance angiography (MRI) · Positron emission tomography (PET) · Ultrasonography (USG)

S. Bano (✉) · S. K. Puri · L. Upreti · H. K. Sant
Department of Radiodiagnosis, Govind Ballabh Pant
Hospital and Maulana Azad Medical College,
New Delhi 110002, India
e-mail: dr_shahinaindia@yahoo.com

S. K. Puri
e-mail: Skpurigbph@yahoo.com

L. Upreti
e-mail: lupreti@rediffmail.co.in

H. K. Sant
e-mail: drhridesh_00@rediffmail.com

V. Chaudhary
Department of Radiodiagnosis,
Employees' State Insurance Corporation (ESIC)
Model Hospital, Gurgaon, Haryana, India
e-mail: dr_vikaschaudhary@yahoo.com

R. Gondal
Department of Pathology, Govind Ballabh Pant Hospital
and Maulana Azad Medical College, New Delhi 110002, India
e-mail: ranjanagondal@yahoo.co.in

Introduction

Gastrointestinal stromal tumors (GISTs), which arise from the interstitial cells of Cajal, are the most common mesenchymal tumors of the gastrointestinal tract. The increasing recognition of GISTs and prolonged survival of the patients with GISTs have made imaging increasingly important not only for diagnosis, but also for monitoring the effects of treatment. Computed tomography (CT) is the imaging modality of choice for these purposes. From July 2006 to March 2010, we reported 22 cases of pathologically and surgically proven GISTs at our hospital. The aim of this retrospective study was to review the imaging features of 22 GIST cases. We also describe the clinical and pathological findings of this well-recognized entity.

Clinical features

Most of the GISTs are small, asymptomatic and discovered incidentally. The reported age of presentation is 40–70 years, with an equal male-to-female ratio [1]. GISTs are very rare in children and young adults, and are sometimes associated with familial disorders, such as neurofibromatosis type 1 [2]. Clinical presentation depends on the site and size of the tumor. The most common presenting symptom includes abdominal pain or a palpable mass, followed by a GI bleed, unexplained anemia, fatigue and malaise. Occasionally, duodenal tumors can present with obstructive jaundice. Despite the large size of the tumor, bowel obstruction is rare. Important complications associated with GISTs are hemorrhage and spontaneous rupture endoluminally or into the peritoneal cavity [1, 3].

Pathologic features

GISTs were previously thought to arise from smooth muscle or Schwann cells, and were classified as leiomyoma, leiomyosarcoma or schwannomas because on light microscopy these tumors share many features. However, the advent of electron microscopy and immunohistochemistry revealed the lack of smooth muscle and Schwann cells in GISTs, and showed expression of c-Kit receptor or CD117. Kit protein is characteristically expressed in Cajal cells, which are GI pacemakers forming the interface between the autonomic nerve endings and the smooth muscle. Thus, CD117 is considered a highly specific marker that differentiates GISTs from other mesenchymal tumors (Fig. 1a). Histologically, these tumors are classified into either spindle or epithelioid cell types (Fig. 1b) [1, 4]. Histological grading of GISTs, to define the risk of malignancy, is based on the number of mitotic figures per high power field (HPF) [3].

Imaging perspective

The aim of imaging is to locate the lesion, define its morphological characteristics, evaluate local invasion and detect distant metastasis. CT is the imaging of choice for these purposes. Multidetector CT can pick up most lesions >2 cm. CT angiography demonstrates prominent feeding and draining vessels to these hypervascular masses. CT is also superior for staging of GISTs and monitoring the disease during and after treatment [5]. MRI is particularly useful in cases where CT is contraindicated, in delineating the rectal GIST and defining its relationship prior to the surgical intervention, and in detecting hemorrhage and necrosis. MRI can better evaluate liver metastasis than CT

[6]. However, CT is superior in demonstrating mesenteric lesions [5]. Ultrasound may also be useful to evaluate the liver metastasis. Endoscopic ultrasonography provides good morphological details of the submucosal GISTs [7]. FDG-PET is highly sensitive in detecting occult GISTs and in the evaluation of treatment response [8]. However, because of the limited availability and high cost, FDG-PET is only indicated when CT findings are inconclusive or inconsistent with the clinical presentation.

GIST can occur anywhere along the gastrointestinal tract, with the stomach, duodenum and small bowel being the most common sites, followed by the large bowel and the esophagus. Extra-gastrointestinal GISTs arising as primary tumor of the pancreas, peritoneum (mesentery and omentum), retroperitoneum or gall bladder occur rarely [9–13]. Of the 22 patients reviewed in our series, 6 (35.5%) had GISTs in the stomach, 5 (17.6%) in the duodenum, 4 (17.6%) in the small bowel, 2 (11.7%) in the large bowel, and 1 (5.88%) each in the esophagus, pancreas, gallbladder, mesentery, peritoneum and the retroperitoneum.

Imaging features of GISTs predominantly depend on the size and aggressive nature of the tumor. At presentation, most GISTs are typically large (>5 cm), hypervascular, heterogeneously enhancing exophytic masses on contrast-enhanced CT. Heterogeneity is because of necrosis, cystic degeneration, hemorrhage or rarely calcification (Figs. 2, 3). Cavitation, ulceration and fistulization to the gastrointestinal lumen are also common features of GISTs. The ulcers and cavities may communicate with the intestinal lumen and contain air, air-fluid level or oral contrast medium (Figs. 4, 5, 6). Duodenal GISTs may cause obstructive jaundice (Fig. 7). The majority of GISTs are well circumscribed, and have smooth or lobulated margins. Irregular surfaces or indistinct margins favor malignancy
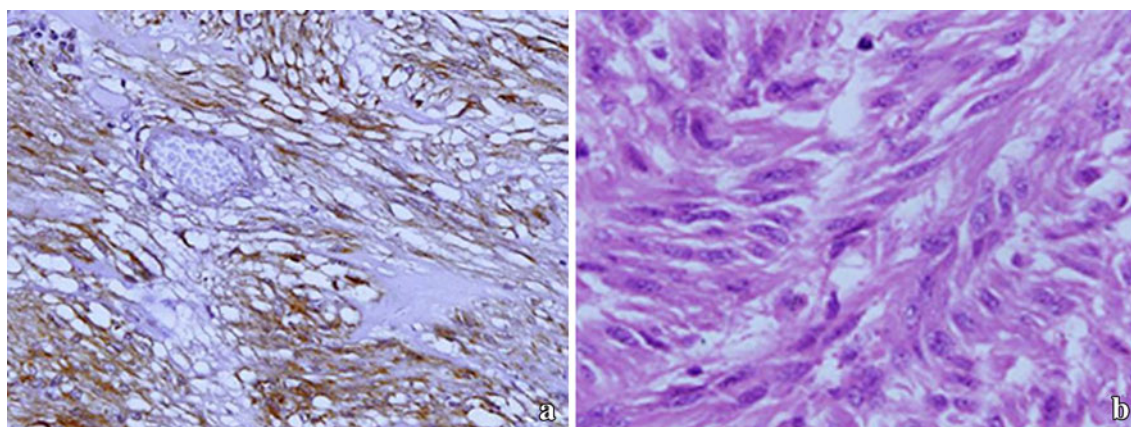

Fig. 1 Photograph of immunohistochemistry (**a**) and histopathology (**b**) slide of gastrointestinal stromal tumor (GIST) showing expression of c-kit (CD 117), diagnostic of a gastrointestinal stromal tumor; and fascicles of spindle cells (H&E stain, ×20 magnification), respectively
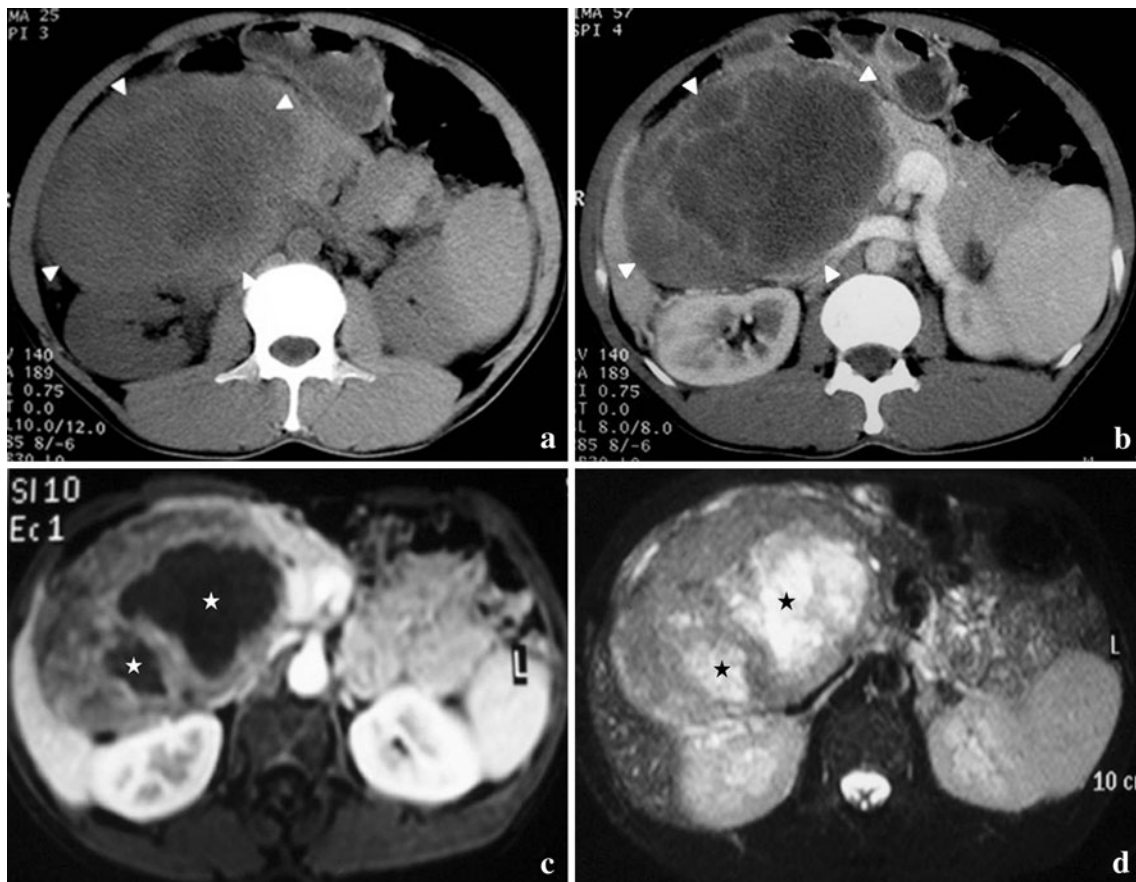
Fig. 2 A 52-year-old male patient with gastrointestinal stromal tumor of the pancreas who presented with upper abdominal pain and a lump. Axial plain (**a**) and contrast-enhanced (**b**) CT scan shows a large, solid, heterogeneously enhancing exophytic mass (*arrowheads*) arising from the head of the pancreas. No dilatation of the pancreatic or biliary duct was noted. On MRI, T1-weighted post-contrast (**c**) and T2-weighted fat-suppressed (**d**) images demonstrate necrosis/cystic degeneration (*asterisk*) within the tumor
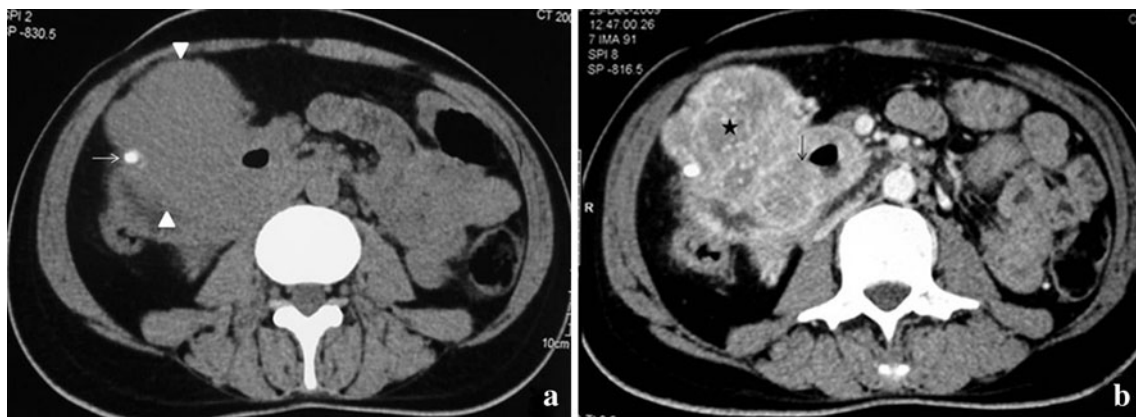

Fig. 3 A 55-year-old male with gastrointestinal stromal tumor of the small bowel who presented with chronic progressive mid-abdominal pain. Axial plain (**a**) and contrast-enhanced (**b**) CT scan images show a large, lobulated, heterogeneously enhancing hypervascular mass arising from the small bowel having both exophytic (*asterisk*) and endoluminal (*black arrow*) components. A dense fleck of calcification is evident at the periphery of the mass (*white arrow*)
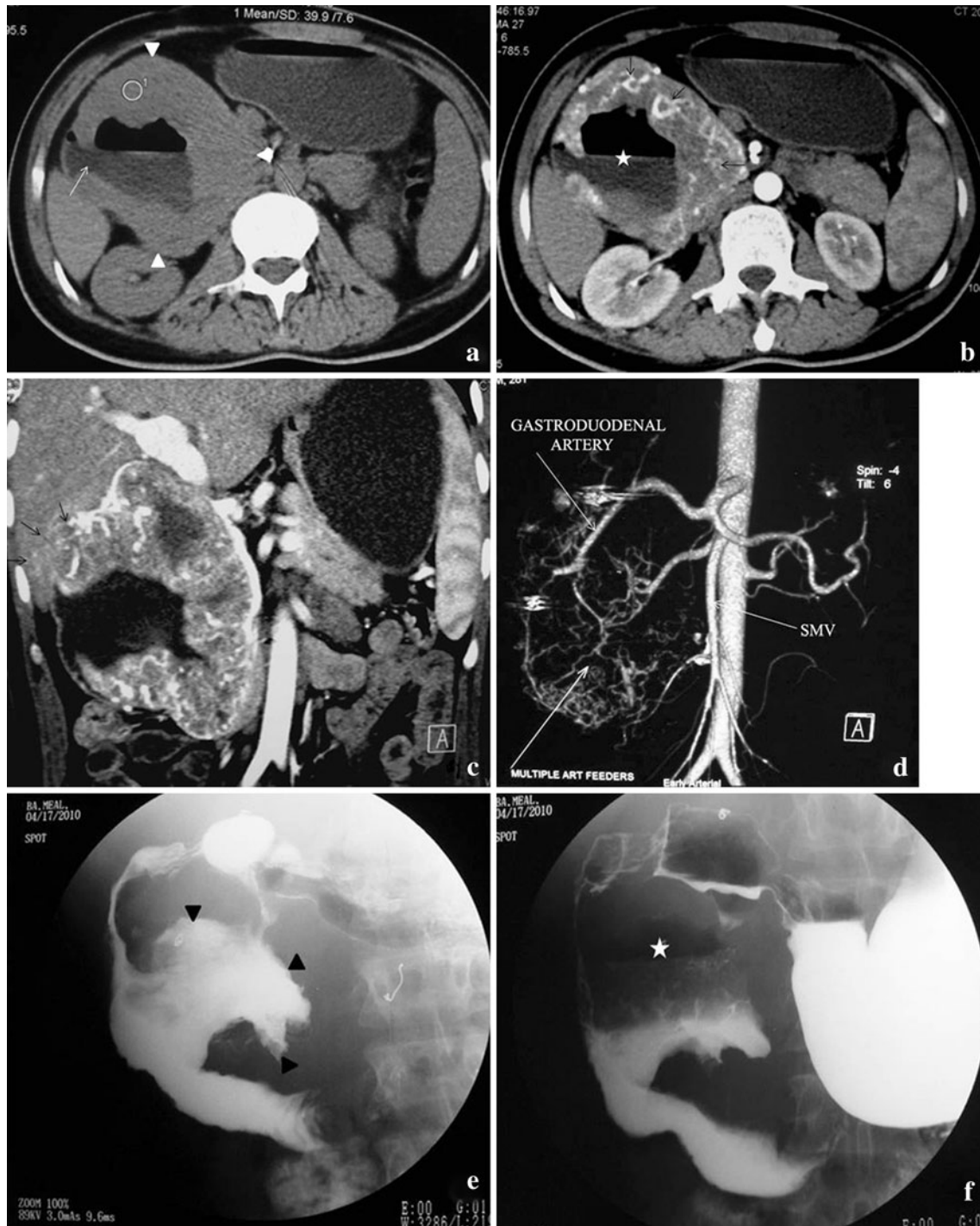
Fig. 4 A 38-year-old male with duodenal gastrointestinal stromal tumor who presented with abdominal pain, obstructive jaundice and upper gastrointestinal bleeding. Axial plain (**a**) and CECT early arterial phase (**b**) images show a large cavitating mass (*arrowheads*) arising from the second part of the duodenum. The cystic cavity communicates (*white arrow*) with the duodenal lumen and contains an air-fluid level (*asterisk*). Multiple intratumoral vessels (*black arrow*) are seen within a solid enhancing portion of the mass. Coronal CECT (**c**) demonstrates peripheral displacement of adjacent bowel loops and vascular structures by the mass lesion. The superior margin of the tumor, in contact with the inferior surface of the liver, is indistinct, and there is loss of the cleavage fat plane between the two, suggesting invasion (*black arrows*). Surgery showed frank invasion of the under surface of the liver. On CT angiography (arterial phase) (**d**), multiple arterial feeders predominantly from the gastroduodenal artery, pancreaticoduodenal arcade and superior mesenteric artery are seen. Barium meal shows oral contrast material within the cavitary duodenal mass (*black arrowhead*) on single contrast supine film (**e**) and air contrast level (*asterisk*) on double contrast erect film (**f**)

Fig. 5 A 45-year-old male with duodenal gastrointestinal stromal tumor who presented with an abdominal mass, pain and upper gastrointestinal bleeding. Axial T1-weighted (**a**) and T2-weighted (**b**) MRI images demonstrate a large, solid soft tissue mass (*arrowheads*) arising from the medial wall of the second part of the duodenum. The tumor is heterogeneous in appearance because of areas of necrosis (*asterisk*), has a slightly irregular and ill-defined margin and an ulcer crater communicating with the duodenal lumen (*black arrow*). T2-weighted coronal image (**c**) demonstrates displacement of adjacent structures (*black arrow*). Marked enhancement and intratumoral vessels (*black arrow*) are evident on T1-weighted post-gadolinium image (**d**). On barium meal single contrast prone oblique view (**e**), oral contrast material seen within the ulcer crater (*white arrow*) is due to fistula to the duodenal lumen. Corresponding FDG PET scan (**f**) shows localized increased activity (*arrow*) in association with the large duodenal GIST
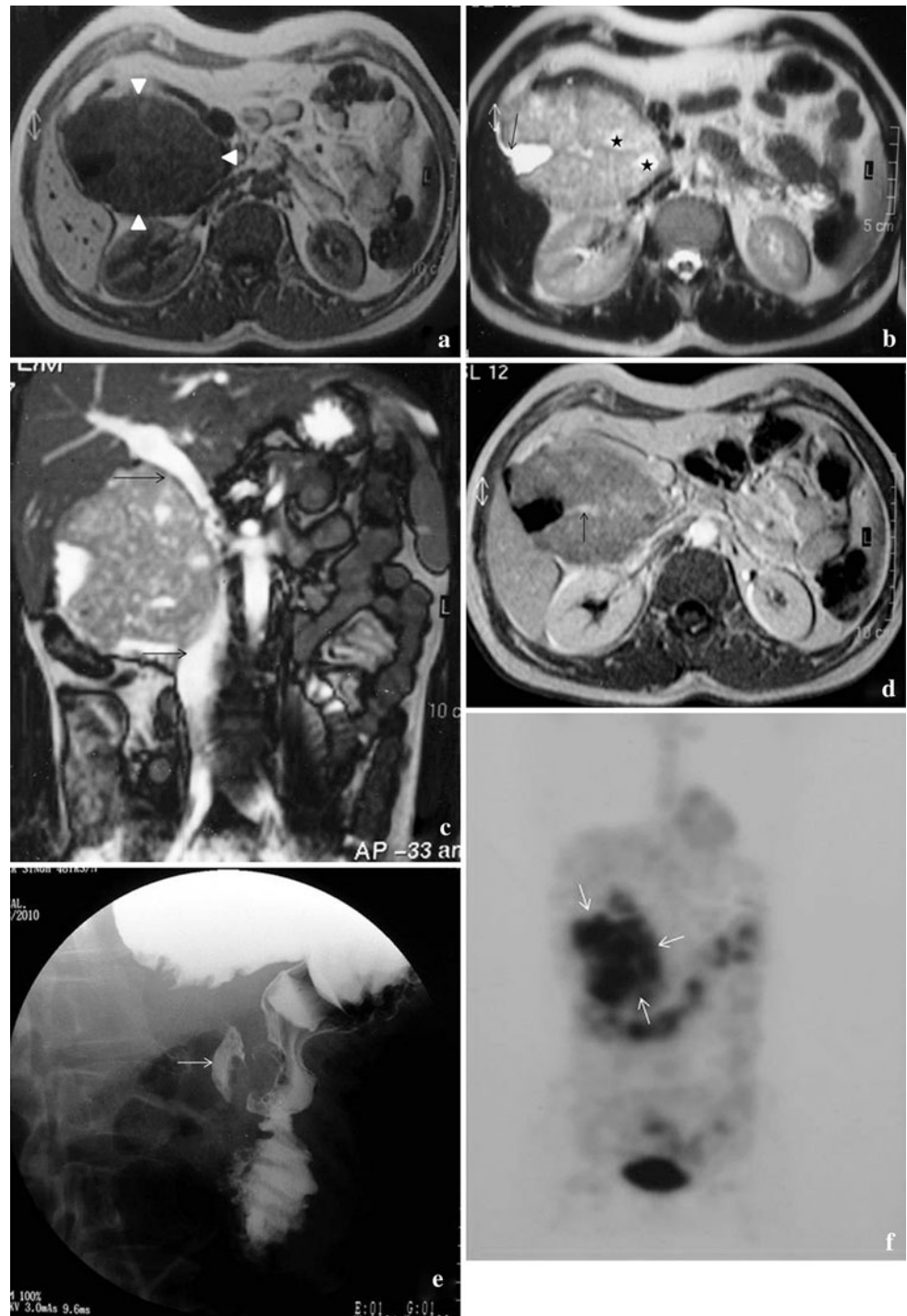
(Figs. 4, 5). The GISTs usually displace the adjacent organs and vessels; however, the invasion of adjacent structures is seen with advanced disease (Figs. 4, 5). GISTs involving the small and large bowel may show aneurysmal dilatation (Fig. 8). This is because the cavitary nature of these tumors produces apparent enlargement of the lumen and may also damage the myenteric plexus causing further dilatation of the lumen. Despite the large size, bowel obstruction is rare, but was seen in one of our cases presenting with rectal GIST (Fig. 9) [1, 8, 14–17]. Primary peritoneal GISTs are often large masses with central low attenuation areas, and appear inseparable from the wall of the stomach or intestine (Fig. 10); however, atypical lesions may mimic peritoneal carcinomatosis demonstrating
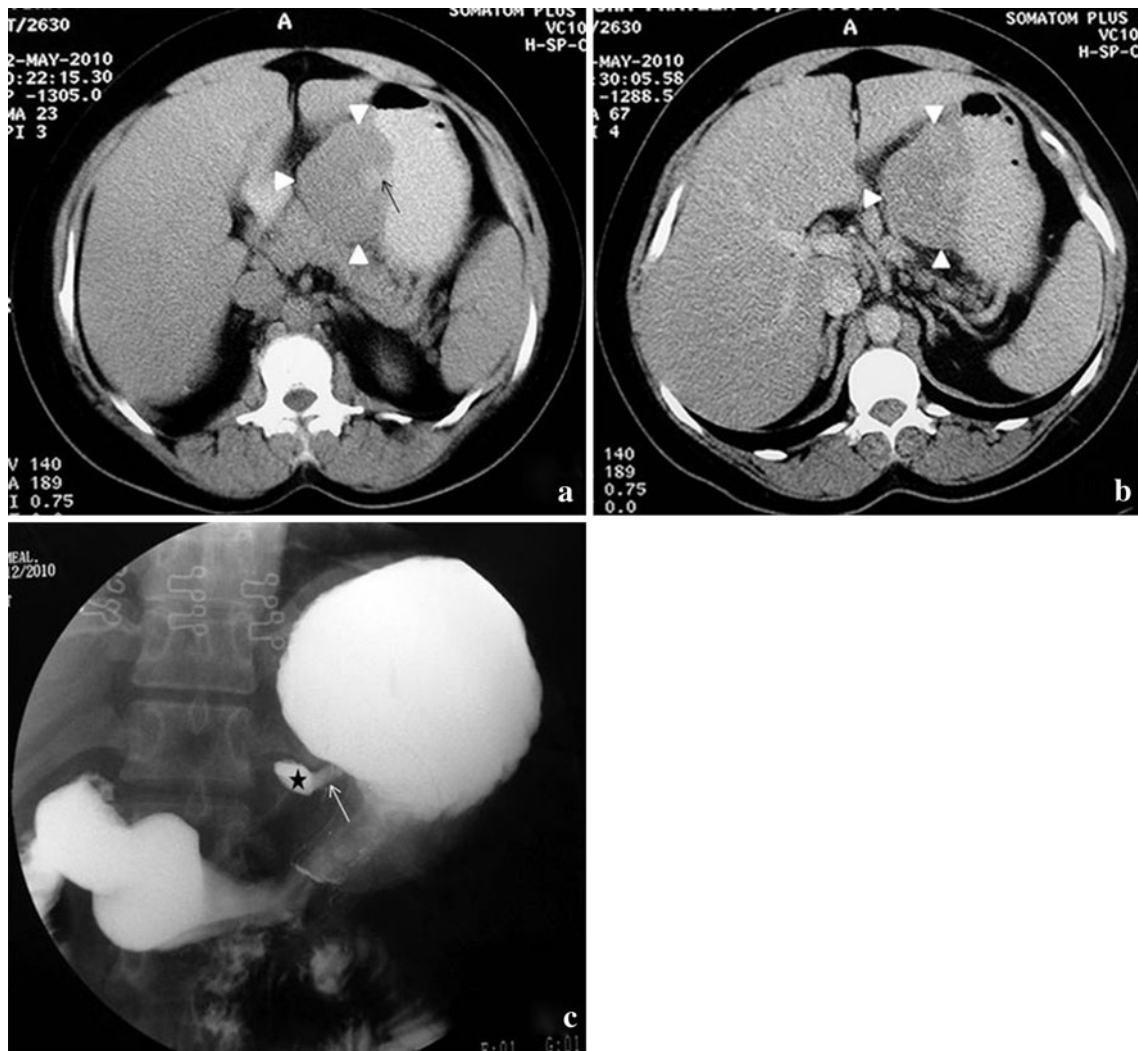
Fig. 6 A 32-year-old female with gastrointestinal tumor of the stomach who presented with epigastric pain, lump and upper gastrointestinal bleeding. Axial plain (**a**) and CECT (**b**) scan shows an exophytic, slightly enhancing soft tissue mass (*arrowheads*) arising from the lesser curvature of the stomach. The oral contrast material within the ulcer crater (*asterisk*) of the mass is due to fistula (*arrow*) to the gastric lumen, which is well documented on single contrast barium meal study (**c**)

variable sized, discrete solid nodules scattered over the omentum and mesentery (Fig. 11) [11, 18]. Pancreatic GISTs have imaging findings similar to those reported with true gastrointestinal GISTs (Fig. 2) [12]. Gall bladder GISTs mimic gall bladder carcinoma and may present as a mass replacing the gall bladder, as focal or diffuse wall thickening, or as an intraluminal polypoidal mass (Fig. 12) [13]. The rarity of ascites has been described in previous reports [16, 18]. Ascites was present in two of our cases, both having peritoneal GISTs (Figs. 10, 11). On post-contrast CT, GISTs often demonstrate intratumoral vessels, dilated feeding arteries or draining veins, suggesting the hypervascular nature of the mass (Fig. 4). No vascular invasion or venous thrombosis has been reported with GISTs [1, 8, 14–17]. PET scan shows increased uptake of ^{18}fluorodeoxyglucose (FDG) by both primary (Fig. 5) and secondary tumor masses.

Small GISTs (<5 cm) are usually asymptomatic and diagnosed incidentally on imaging or endoscopy. These are seen as submucosal or endoluminal polypoidal growths with homogenous contrast enhancement (Figs. 13, 14) [5, 8, 9]. Although many authors have documented the presence of incidental small GISTs, no report on the real incidence of small GISTs is available. Agaimy et al. [19] and Kawanowa et al. [20] have reported 'micro-GISTs' in up to 50% of specimens of gastrectomies performed for other causes.

The liver and peritoneum are the most common sites of metastasis; less commonly, the lung, pleura, bones and soft tissue may be involved [7, 8, 15, 16]. These
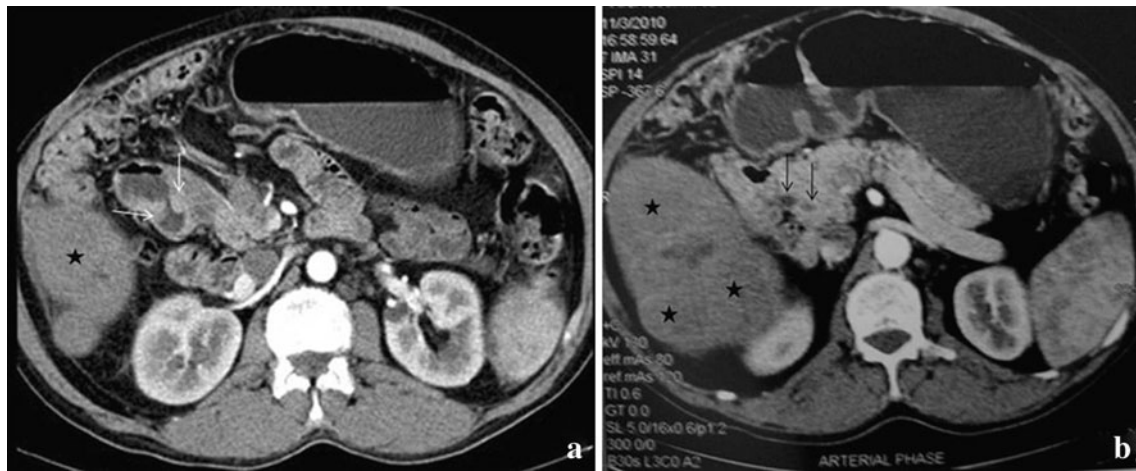
Fig. 7 A 52-year-old male of NF-1 with recurrent gastrointestinal stromal tumor of the duodenum who presented with abdominal pain and jaundice. Axial CECT shows two small endoluminal masses (*white arrows*) in the second part of the duodenum, one in the periampullary region and the other in the opposite duodenal wall (**a**) producing obstructive dilatation of the common bile duct and pancreatic duct (*black arrow*). In addition, multiple liver metastases (*asterisk*) are also evident. The liver metastases demonstrate a mildly enhancing thin peripheral rim with a low density center (**b**)

Fig. 8 A 57-year-old male with gastrointestinal stromal tumor of the small bowel who presented with chronic progressive mid-abdominal pain. Axial plain (**a**) and CECT (**b**) images show a large mass (*arrowheads*) arising from the small bowel, causing aneurysmal dilatation of the bowel (*asterisk*). Intratumoral vessels (*black arrow*) are also evident. On coronal CECT (**c**) proximal and distal segments of the small bowel are of normal caliber (*black arrows*)

tumors characteristically do not show lymphadenopathy [21]. The CT characteristics of metastatic lesions are similar to the primary tumor. The majority of metastases are hypervascular with a low density center (Figs. 7, 15), but hypovascular metastases are also known [7, 8, 15, 16].
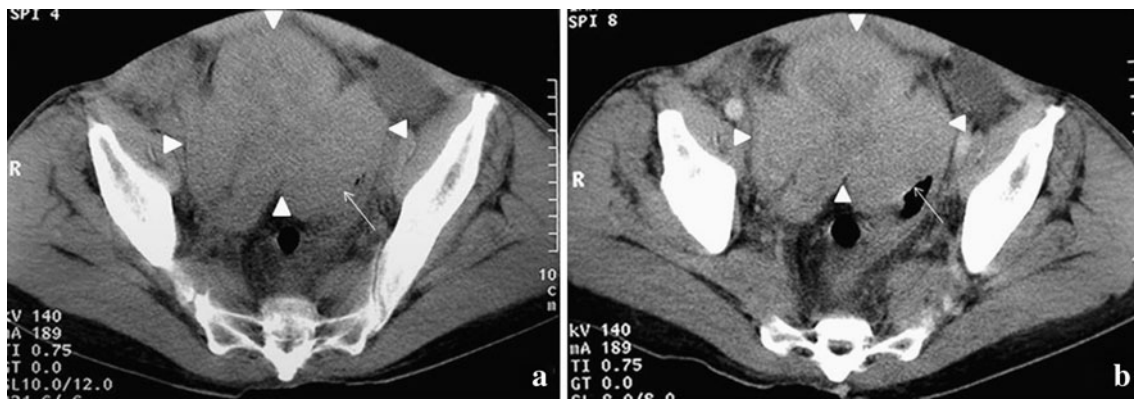
Fig. 9 A 64-year-old male with gastrointestinal stromal tumor of the rectum presenting with chronic back pain and worsening constipation. Axial plain (**a**) and contrast-enhanced (**b**) CT images show a large, trilobulated, moderately enhancing exophytic soft tissue mass arising from the rectum, causing luminal obstruction (*white arrow*)

Fig. 10 A 55-year-old male with typical mesenteric gastrointestinal stromal tumor who presented with a large abdominal lump and abdominal pain. Axial plain (**a**) and CECT (**b**) images demonstrate a large, lobulated, heterogeneously enhancing mesenteric mass (*arrowheads*) with a large area of central necrosis (*asterisk*). Coronal CECT (**c**) and T2-weighted MRI (**d**) images demonstrate peripheral displacement of bowel and vascular structures. A few small intratumoral vessels (*black arrows*) are also evident in the peripheral portion of the mass. Mesenteric vessel thrombosis and mesenteric lymphadenopathy are characteristically absent; however, mild ascites (*asterisk*) is present
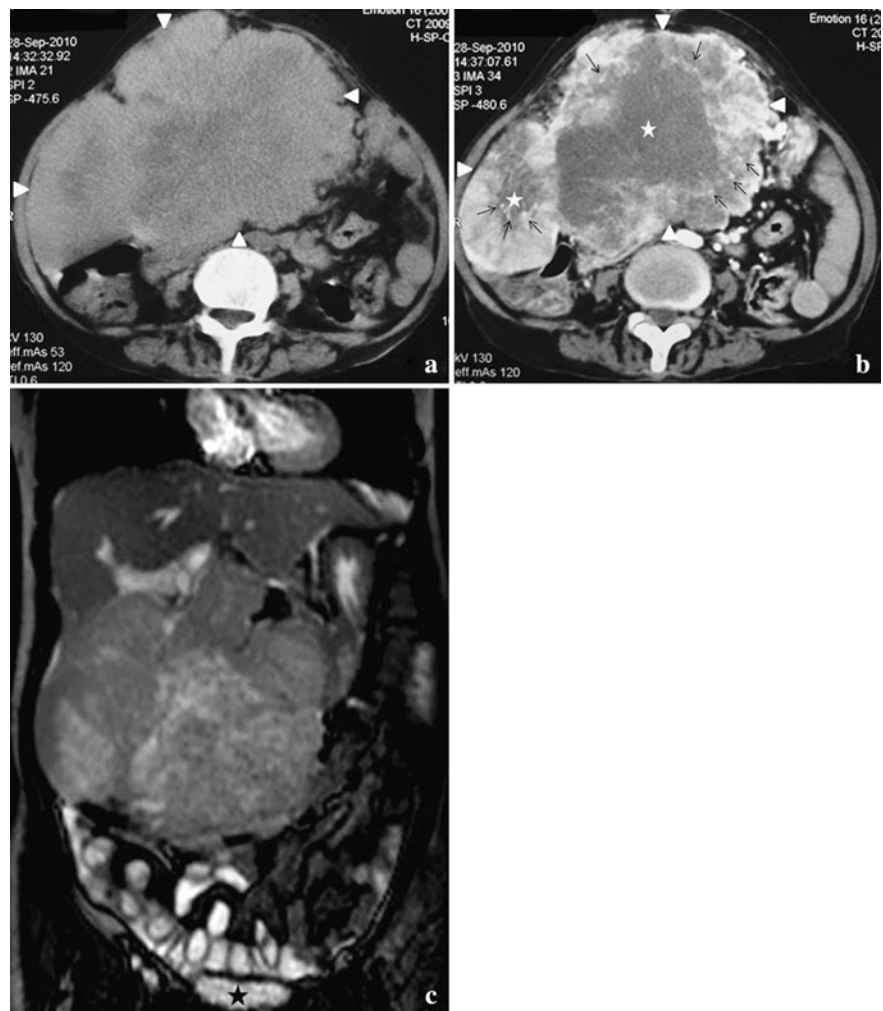
CT findings favoring malignant GISTs include size >5 cm, irregular or indistinct margins, heterogeneous contrast enhancement, local invasion, hematogenous liver or peritoneal metastasis [9, 15, 16]. The two most important parameters that define the malignant nature of the tumor are the tumor size and number of mitotic figures per
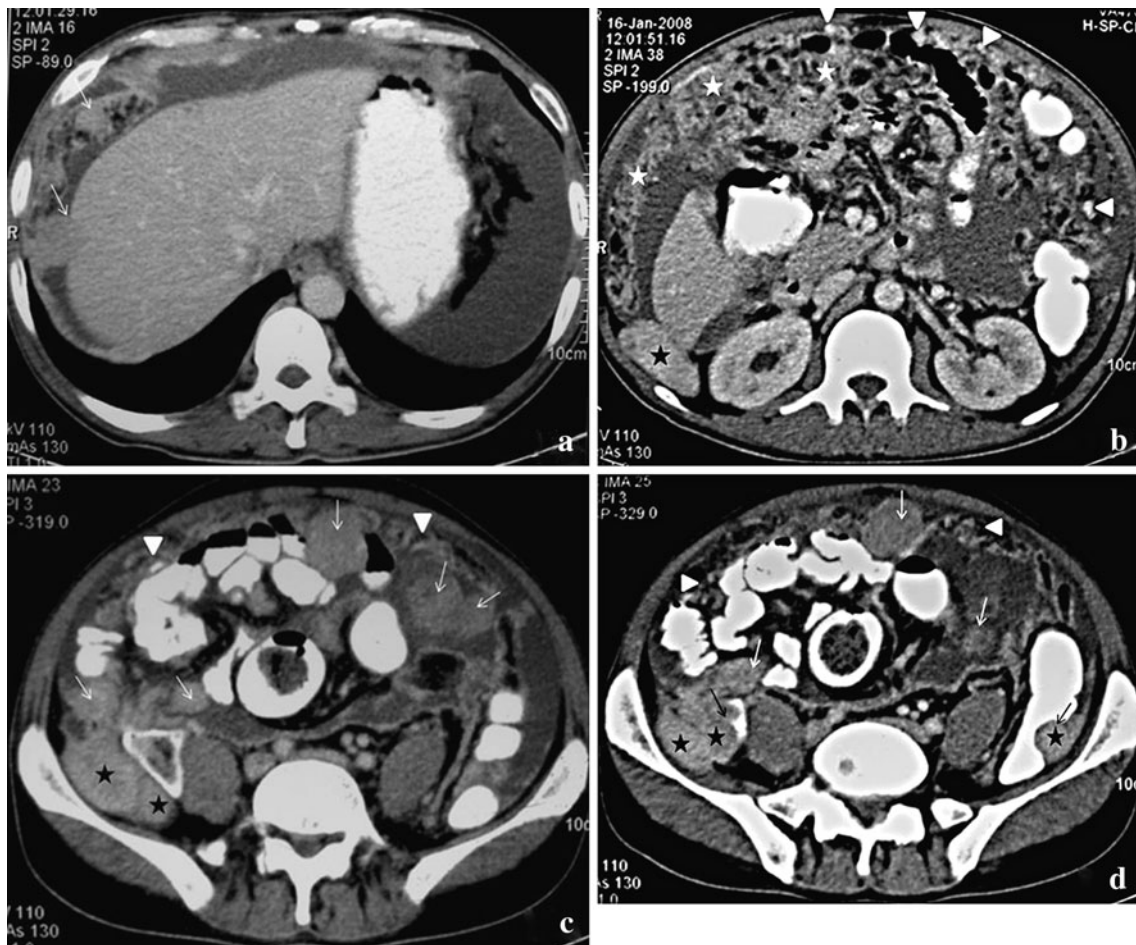
Fig. 11 A 50-year-old male with atypical primary peritoneal and retroperitoneal gastrointestinal stromal tumor mimicking peritoneal carcinomatosis. Axial CECT image of the abdomen (**a–d**) shows multiple, small, variable-sized, discrete, solid nodules scattered predominantly within the peritoneal cavity and scarcely in the retroperitoneum. The majority of these lesions show homogenous contrast enhancement with a few exceptions that demonstrate heterogeneous enhancement. Image at the level of the upper abdomen (**a**) shows nodular lesions (*white arrow*) involving the omentum and visceral surface of the liver. Image at the mid-abdomen level (**b**) shows omental caking (*white asterisk*) and one mass in the right posterior perirenal space adjacent to the lateral aspect of the right kidney, suggesting retroperitoneal deposit (*black asterisk*). Image at the level of the lower abdomen (**c**) shows multiple mesenteric masses (*white arrow*) and retroperitoneal tumor nodules (*black asterisk*) closely abutting the lateral aspect of the cecum. Retroperitoneal lesions (*black asterisk*) are also seen along the lateral aspect of the lower ascending and descending colon, indenting and protruding (*black arrow*) within the bowel lumen (**d**). There is no indrawing or spiculation of the mesentery by the mesenteric masses; however, dilated vascular structures (*arrowheads*) evident at the periphery of the abdomen (**a–d**) represent the hypervascular nature of the mesenteric masses. Gross ascites is also evident

HPFs on histology. Tumors larger than 5 cm with more than 5 mitotic counts per 50 HPF and tumors larger than 10 cm, regardless of the mitotic count, have a high risk of malignancy [22].

Complete surgical resection of the tumor is the treatment of choice. Recently, a new agent, imatinib mesylate (Gleevec, Novartis), which selectively inhibits the enzyme c-Kit tyrosine kinase, has been approved for unresectable or metastatic disease. On follow-up CT scan following i-matinib mesylate, both the primary tumor and the metastases show reduction in size and become homogeneously hypoattenuating within a month because of myxoid degeneration. Development of a fresh enhancing nodule within the treated primary or metastatic lesion suggests recurrence [8]. A high recurrence rate (40–90%) has been documented with GISTs with median duration of about 2 years. Recurrence typically occurs in the liver and peritoneum [23].

The differential diagnosis of the GISTs should be made according to tumor location. Important differentials of gastric GISTs include other mesenchymal tumors such as leiomyomas, leiomyosarcomas, schwannomas, neurofibromas
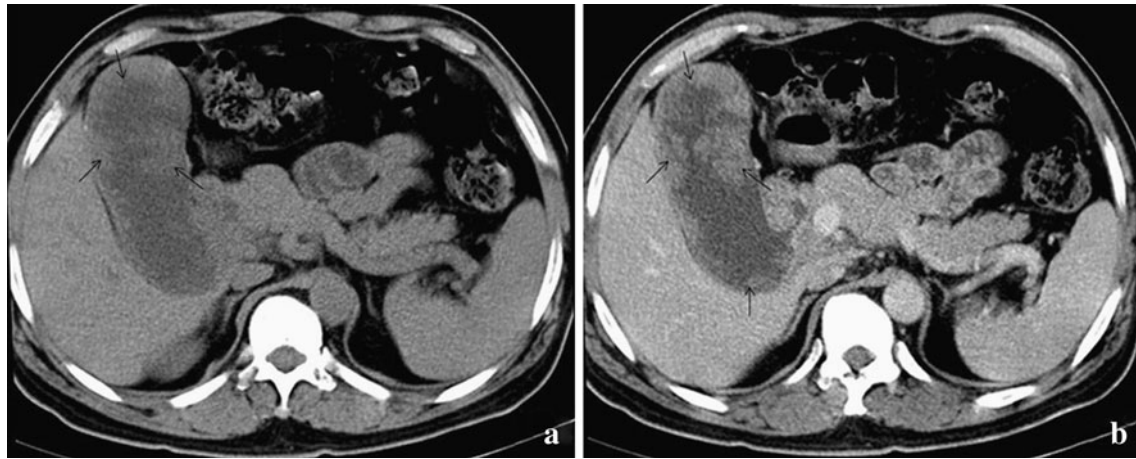
Fig. 12 A 52-year-old female with a gastrointestinal stromal tumor involving the gall bladder who presented with right-sided abdominal pain and vomiting. Axial plain (**a**) and contrast enhanced (**b**) CT scan shows a moderately distended gall bladder with diffuse, asymmetric, nodular wall thickening (*arrow*). No regional lymphadenopathy, intraluminal calculus or cystic/common bile duct obstruction was noted

Fig. 13 A 45-year-old male with esophageal gastrointestinal tumor who presented with dysphagia. Axial contrast-enhanced CT shows a small, lobulated, homogenous, moderately enhancing, submucosal mass (*arrow*) involving the mid-thoracic esophagus causing luminal narrowing
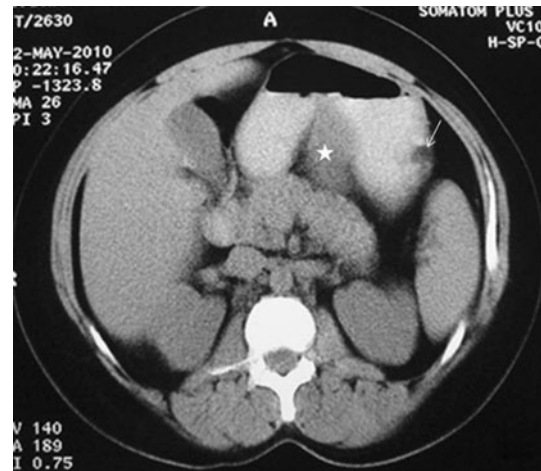

Fig. 14 A 32-year-old female (same as in Fig. 6) with gastrointestinal stromal tumors of the stomach. Axial plain CT with oral contrast shows another small endoluminal polypoidal growth arising from the greater curvature [in addition to the large exophytic mass (*asterisk*) arising from the lesser curvature as shown in Fig. 6]

and neuroendocrine tumors. The imaging findings of these tumors are similar to the GISTs, and the differentiation is only possible on histopathology and immunohistochemistry [7, 9, 16]. The differential diagnosis of small and large bowel GISTs includes adenocarcinoma and lymphoma. Adenocarcinomas and lymphomas commonly have associated regional lymphadenopathy, which is characteristically absent in GISTs. Unlike adenocarcinoma, GISTs involve the bowel eccentrically; as a result bowel obstruction is rare. Like lymphoma, GISTs may also show aneurysmal dilatation of the bowel [7, 16]. Primary or metastatic peritoneal GISTs are differentiated from peritoneal tuberculosis and peritoneal carcinomatosis. The mesenteric and omental masses in case of GISTs are usually well defined with smooth surfaces, and do not show spiculation or indrawing of the mesentery. The rarity of ascites and dilated feeding arteries or draining veins on CT further favors GISTs over tubercular peritonitis or peritoneal carcinomatosis [11, 18]. Gall bladder sarcomas are differentiated from gallbladder carcinoma on the basis of the absence of lymphadenopathy and cytohistopathology [13].

CT is the imaging modality of choice for diagnosing GIST at initial presentation, staging and monitoring the disease during and after the treatment. Radiologists can often predict the correct diagnosis at presentation by the appearance of a large exophytic gastrointestinal mass without significant lymphadenopathy. Adenopathy, concentric bowel involvement, large-volume ascites and spiculated mesenteric masses suggest an alternative diagnosis.

Fig. 15 A 62-year-old male (another patient) with gastrointestinal stromal tumor of the rectum. Axial contrast-enhanced CT (arterial phase) image demonstrates multiple hypervascular liver metastases (*arrowheads*) with central necrosis

References

1. Sandrasegaran K, Rajesh A, Rydberg J, Rushing AD, Faith MA, Henley JD. Gastointestinal stromal tumors: clinical, radiologic, and pathologic features. AJR. 2005;184:803–11.
2. Behrenwala KA, Spalding D, Wotherspoon A, Fisher C, Thompson JN. Small bowel gastrointestinal stromal tumors and ampullary cancer in type I neurofibromatosis. World J Surg Oncol. 2004;7:1–4.
3. Pidhorecky I, Cheney RT, Kraybill WG, Gibbs JF. Gastrointestinal stromal tumors: current diagnosis, biologic behavior, and management. Ann Surg Oncol. 2000;7:705–12.
4. Hasegawa T, Matsuno Y, Shimoda T, Hirohashi S. Gastrointestinal stromal tumor: consistent CD117 immunostaining for diagnosis, and prognostic classification based on tumor size and MIB-1 grade. Hum Pathol. 2002;33:669–76.
5. Nishida T, Kumano S, Sugiura T, Ikushima H, Nishikawa K, Ito T, et al. Multidetector CT of high risk patients with occult gastro intestinal stromal tumors. AJR. 2003;180:185–9.
6. Hasegawa S, Semelka RC, Noone TC, Woosley JT, Marcos HB, Kenney PJ, et al. Gastric stromal sarcomas: correlation of MR Imaging and histopathological findings in nine patients. Radiology. 1998;208:591–5.
7. Ulusan S, Koc Z, Kayaselcuk F. Imaging characteristics of liver metastasis from gastrointestinal stromal tumor and after imatinib mesylate treatment. Turk J Gastroenterol. 2008;19(2):129–32.
8. Choi H, Charnsangavej C, de Castro Faria S, Tamm EP, Benjamin RS, Johnson MM, et al. CT evaluation of the response of gastrointestinal stromal tumors after imatinib mesylate treatment: a quantitative analysis correlated with FDG PET findings. AJR. 2004;183:1619–28.
9. Kim HC, Lee JM, Kim KW, Park SH, Kim SH, Lee JY, et al. Gastrointestinal stromal tumors of the stomach: CT findings and prediction of malignancy. AJR. 2004;183:893–8.
10. Wong CS, Chan T, Chu YC, Cheng LF, Mak YF, Lee KY, et al. Oesophageal gastro-intestinal stromal tumor presenting with rupture into pleural cavity. Hong Kong Med J. 2007;13:478–81.
11. Kim HC, Lee JM, Kim KW, Park SH, Kim SH, Lee JY, et al. Primary gastrointestinal stromal tumors in the omentum and mesentery: CT findings and pathologic correlations. AJR. 2004;182:1463–7.
12. Trabelsi A, Ben Yacoub-Abid L, Mtimet A, Abdelkrim SB, Hammedi F, Ali AB, et al. Gastrointestinal stromal tumor of the pancreas: a case report with review of the literature. North Am J Med Sci. 2009;1:324–6.
13. Peerlinck IDL, Irvin TT, Sarsfield PTL, Harington JM. GIST (gastro-intestinal stromal tumor) of the gallbladder: a case report. Acta Chir Belg. 2004;104:107–9.
14. Levy AD, Remotti HE, Thompson WM, Sobin LH, Miettinem M. Gastrointestinal stromal tumors: radiologic features with pathologic correlation. RadioGraphics. 2003;23:283–304.
15. Ulusan S, Koc Z. Radiologic findings in malignant gastrointestinal stromal tumors. Diagn Interv Radiol. 2009;15:121–6.
16. Burkill GJ, Badran M, Al-Muderis O, Meirion TJ, Judson IR, Fisher C, et al. Malignant gastrointestinal stromal tumor: distribution, imaging features, and pattern of metastatic spread. Radiology. 2003;226:527–32.
17. Lee CM, Chen HC, Leung TK, Chen YY. Gastrointestinal stromal tumor: computed tomographic features. World J Gastroenterol. 2004;10(16):2417–8.
18. Yang TH, Hwang JI, Hung SW, Wang RC, Lee M, Kim YJ, et al. Gastrointestinal stromal tumor of the omentum and mesentery mimicking peritoneal carcinomatosis: a case report. Chin J Radiol. 2006;31:53–8.
19. Agaimy A, Wunsch PH, Hofstaedter F, Blaszyk H, Rummele P, Gaumann A, et al. Minute gastric sclerosing stromal tumors (GIST tumorlets) are common in adults and frequently show c-KIT mutations. Am J Surg Pathol. 2007;31(1):113–20.
20. Kawanowa K, Sakuma Y, Sakurai S, Hishima T, Iwasaki Y, Saito K, et al. High incidence of microscopic gastrointestinal stromal tumors in the stomach. Hum Pathol. 2006;37:1527–1.
21. Berman J, O'Leary TJ. Gastrointestinal stromal tumor workshop. Hum Pathol. 2001;32:578–82.
22. Fletcher CDM, Berman JJ, Corless C, Gorstein F, Lasota J, Longley BJ, et al. Diagnosis of gastrointestinal stromal rumors: a consensus approach. Hum Pathol. 2002;33:459–65.
23. Dematteo RP, Lewis JJ, Leung D, Mudan SS, Woodruff JM, Brennan MF. Two hundred gastrointestinal stromal tumors: recurrence patterns and prognostic factors for survival. Ann Surg. 2000;231:51–8.